Phytomedicine Plus 1 (2021) 100014

Contents lists available at ScienceDirect

Phytomedicine Plus

journal homepage: www.elsevier.com/locate/phyplu

Moringa oleifera leaf extract influences oxidative metabolism in C2C12 myotubes through SIRT1-PPARα pathway

Guglielmo Duranti[a,*], Mariateresa Maldini[b], Domenico Crognale[c], Stefania Sabatini[a], Federica Corana[d], Katy Horner[c], Roberta Ceci[a]

[a] *Laboratory of Biochemistry and Molecular Biology - Department of Movement, Human and Health Sciences, Università degli Studi di Roma "Foro Italico", Piazza Lauro De Bosis 6, Roma 00135, Italy*
[b] *SCIEX Italia S.r.L., Via Montenapoleone, 8, 20121 Milano, MI, Italy*
[c] *Institute for Sport & Health, School of Public Health, Physiotherapy and Sports Science, University College Dublin, D04 V1W8 Dublin 4, Dublin, Ireland*
[d] *Centro Grandi Strumenti, Università degli Studi di Pavia, Via Bassi 21, 27100 Pavia, PV, Italy*

ARTICLE INFO

Keywords:
Moringa oleifera leaf extract (MOLE)
Skeletal muscle
Energy metabolism

ABSTRACT

Background: *Moringa oleifera* is an important traditional multipurpose plant, due to the presence of many bioactive compounds. *Moringa oleifera* leaf extracts (MOLE) have been shown to have many beneficial properties in pathological conditions including diabete. However, the lack of information about its exact molecular mechanism of action might hinder other potential use in different areas such as skeletal muscle physiology.

Hypothesis/purpose: Skeletal muscle represents about 40-50% of the total mass of a lean individual and is an insulin-sensitive tissue with wide variations in energy requirements. We aimed to test the effects of MOLE on oxidative metabolism and the molecular mechanism involved on myotubes by using C2C12 cell line, a well known model for in vitro skeletal muscle studies.

Study design: C2C12 myotubes were treated with MOLE at different working solutions for 24 and 48 hours and then culture media and cellular extracts were collected. MOLE was screened for phytochemicals determination.

Methods: Glucose and free fatty acids consumption along with lactate release were assessed in the culture media. Citrate sinthase, 3-hydroxy acylCoA dehydrogenase, alanine transglutaminase and creatine kinase enzyme activities, as well as the metabolic regulatory SIRT1 and PPARα protein levels were evaluated in cellular extracts.

Results: MOLE administration induced a dose and time dependent increase in substrates consumption accompanied by an increase in intracellular oxidative metabolism enzymatic activity levels. The extracts were also able to modulate positively the protein expression of SIRT1 and PPARα.

Conclusion: Altogether, these data indicate that MOLE could represent a valid nutritional support for improving skeletal muscle metabolism: in fact MOLE treatment increased oxidative energy metabolism and possibly favours mitochondrial biogenesis through SIRT1/PPARα pathway. future studies will clarify wether *Moringa oleifera* leaf extracts consumption may be useful to improve physical performance and metabolic-related skeletal muscle diseases.

Introduction

The impaired ability of insulin to stimulate glucose uptake and utilization is a common physiological condition of type 2 diabetes and counteracting insulin resistance is an important therapeutic target in the management of the disease (De Fronzo and Tripathy, 2009).

Plant-derived extracts are abundant in bioactive molecules, and some of them have shown pharmacological properties in the treatment of diabetes (Xu et al., 2018).

Abbreviations: ALT, alanine transglutaminase; CK, creatine kinase; CS, citrate sinthase; FFAs, free fatty acids; GLU, glucose; GLUT4, glucose transporter 4; HAD, 3-hydroxy acylCoA dehydrogenase; LAC, lactate; LDH, lactate dehydrogenase; MAPK, mitogen-activated protein kinase; MOLE, methanolic *Moringa oleifera* leaf extract; MTT, methylthiazolyldiphenyl-tetrazolium bromide; PGC1α, PPAR gamma coactivator 1; PPARα, peroxisome proliferator-activated receptor alpha; SIRT1, silent mating type information regulator 2 homolog 1; TAC, Trolox®-equivalents Antioxidant Capacity.

* Corresponding author.
E-mail address: guglielmo.duranti@uniroma4.it (G. Duranti).

https://doi.org/10.1016/j.phyplu.2020.100014
Received 5 November 2020; Received in revised form 17 December 2020; Accepted 22 December 2020

Among these, the beneficial properties of *Moringa oleifera* are continuously emerging and its use in various physiological conditions and diseases including insulin resistance and diabetes has been investigated (Nova et al., 2020). Leaves, stems, roots, flowers and seeds, have shown multiple nutraceutical or pharmacological functions. Many of the bioactive components characterizing *Moringa oleifera* are used for different industrial and food applications due to their anti-inflammatory, antioxidant, anti-cancer, hypoglycemic, and blood lipid-reducing functions (Manohar et al., 2012; Stohs and Hartman, 2015; Kuo et al., 2018).

Among the bioactive compounds present, phenolic acids and in particular chlorogenic and ferulic acid, together with flavonoids such as quercetin, vanillin and kaempferol, appear the most beneficial molecules (Saucedo-Pompa et al., 2018). Leaf extracts have shown significant anti-hyperglycemic and hypoglycemic activity in healthy and diabetic rat models (Nahar et al., 2016).

Moreover, methanolic leaf extract treatment has demonstrated a remarkable reduction in total cholesterol, triglycerides, and body weight, moreover, liver biomarkers, organ weight, and blood glucose levels were also decreased in hypercholesterolemic rats (Bais et al., 2014).

Despite many studies on *Moringa oleifera* extracts performed in animals, at present there is no information about the molecular mechanism through which MOLE influences energy metabolism.

Skeletal muscle constitutes up to 50% of total body mass, it plays an important role in the regulation of nutrients (Sinacore and Gulve, 1993) and the rapid changes in fuel selection constitute a hallmark for metabolically healthy muscle.

There are different pathways that can be activated to fulfill the skeletal muscle energy request. Between them, the activation of oxidative metabolism can involve the activation of the MAPK-SIRT1-PGC1α axis (Pardo and Boriek, 2011). The mitogen-activated protein kinase (MAPK) is an upstream regulator of sirtuin 1 (silent mating type information regulator 2 homolog 1 - SIRT1). SIRT1 is a key molecule in metabolic regulation through its ability to deacetylate and activate the PPAR gamma coactivator 1 alpha (PGC1α), a transcription co-regulator of peroxisome proliferator-activated receptors (PPARs), with the final result of increasing mitochondrial biogenesis and oxidative metabolism (Wu et al., 1999; Ferrè, 2004; Pardo and Boriek, 2011).

Among the latter, PPAR alpha (PPARα) is present in skeletal muscle and liver, which is closely correlated with fatty acid oxidation and has been suggested as an important therapeutic target for metabolic diseases with hyperlipidemia (Stec et al., 2019).

An increase of mitochondrial oxidative metabolism involves the positive modulation of citrate synthase (CS), the key enzyme of the Krebs cycle, and 3-hydroxy acyl- CoA dehydrogenase (HAD), the third enzyme in the process of fatty acid β-oxidation (Sabatini et al., 2011). The increase in the oxidative enzymes lead to mithochondrial biogenesis and, very often, to an overall increase muscle mass that can be assessed by the evaluation of creatine kinase (CK) activity (Watchko et al., 1996; Zanou and Gailly, 2013).

In order to evaluate the molecular mechanism involved in the *Moringa oleifera* action, the present study was designed to assess the effect of 24 and 48 hours treatment at different working solutions on energy metabolism in the mouse C2C12 cell line, a well-known model for in vitro skeletal muscle studies. In C2C12 myotubes we evaluated: substrate consumption (culture media glucose (GLU), free fatty acids (FFAs) and lactate (LAC) levels); key metabolic enzyme activities (lactate dahydrogenase (LDH), citrate sinthase (CS), 3-hydroxy acylCoA dehydrogenase (HAD), alanine transglutaminase (ALT) and creatine kinase (CK)); glucose transporter GLUT4, the metabolic regulatory SIRT1 and PPARα protein levels were also assessed.

Materials and methods

All chemical reagents, unless otherwise specified, were purchased from Sigma-Aldrich Chemical (St. Louis, MO, USA).

Methanolic extract of Moringa oleifera leaves (MOLE)

One gram of *Moringa oleifera* leaf powder (PureBodhi Nutraceuticals Ltd, UK) was sonicated (Vibra-Cell CV 18 SONICS VX 11, Sonics & Materials, CT, USA) in 10 mL of methanol 100% twice for 10 min at +4°C. After the ultrasonic treatment, the extract were centrifuged (2000 x g for 10 minutes at +4°C) and the methanolic extract (stock solution) was collected, then tested for the evaluation of the antioxidant capacity and stored at -20°C.

Ultra-high performance liquid chromatographic and high resolution mass spectrometric conditions (UHPLC-QTOF)

To obtain a metabolomic fingerprint of MOLE, UHPLC-QTOF analysis was performed. 10 μL of diluted extract (1:10; v/v with buffer A) was directly injected using an ExionLC^{TM} AD system interfaced to a High Resolution SCIEX X500B QTOF mass spectrometer. Separation was performed using a Phenomenex Luna Omega Polar C18 (150 × 4.6 mm, 3 μm) analytical column. The column oven was maintained at 40°C and the elution solvents consisted of 0.1% formic acid in water (buffer A) and 0.1% formic acid in acetonitrile (buffer B) at a flow-rate of 0.8 mL/min. The following gradient was used: 0 min- 5% buffer B, 16 min-45% buffer B, 21min-80% buffer B; 22 min-100% buffer B.

The high-resolution SCIEX X500B QTOF mass spectrometer was working with an electrospray ion source operating in negative ion mode. SWATH analysis was carried out as election acquisition method since it is able to provide a digital fingerprint of sample. Being a data independent acquisition strategy (SWATH), high resolution precursor and product spectral information for all detectable constituents in the sample were collected. 25 SWATH variable windows were utilized to obtain high quality MS/MS spectra, the accumulation for the TOF MS is 0.150 sec and the accumulation time for the TOF MS/MS is 0.025 sec. The following MS source conditions were used: CUR=40 psi, CAD=11, IS =-4500 V, TEM=450°C, GS1= 65 psi and GS2= 60 psi.

Data Processing: Data were processed using SCIEX OS Software 2.0. The SCIEX Natural Products 2.0 Library was used for searching database compound spectra for matches to experimentally derived spectra.

Trolox® equivalents antioxidant capacity (TAC)

Trolox® equivalents antioxidant capacity of MOLE was evaluated spectrophotometrically, as previously described (Duranti et al., 2017). This assay evaluates the ability of MOLE in preventing $ABTS^{\cdot+}$ radical formation, compared to Trolox® (vitamin E analogue) standards. Briefly, 10 μL of MOLE stock solution dilutions (1/1000–1/500–1/100 and 1/10 working solution) or Trolox® standards (0.25–0.5–1.0 mM) were incubated in ABTS-met-Myo-PBS buffer and the absorbance at 734 nm was monitored for 2 min. The reaction was started by the addiction of H_2O_2 (450 μM), followed for 10 min, and the variation of absorbance was then recorded. Sample $\Delta OD/min_{734}$ was compared to those obtained using Trolox® standards.

Cell culture

C2C12 myoblasts (2×10^3 cm^2; ATCC, Manassas, VA, USA) were cultured as previously described (Duranti et al., 2017). Differentiation into myotubes was achieved by culturing preconfluent cells (85% confluency) in medium containing 2% FBS and monitoring them by microscopy and for myogenin expression by western blot analysis. Cells were treated with working solution 1/1000 or 1/100 MOLE or vehicle (methanol) in culture media for 24 and 48 hours. Insulin (100 nM) was utilized as positive control (Yang et al., 2012). Methylthiazolyldiphenyltetrazolium bromide (MTT) assay at 24- and 48-hours treatment were performed and no statistical significant differences were found compared to untreated cells (data not shown).

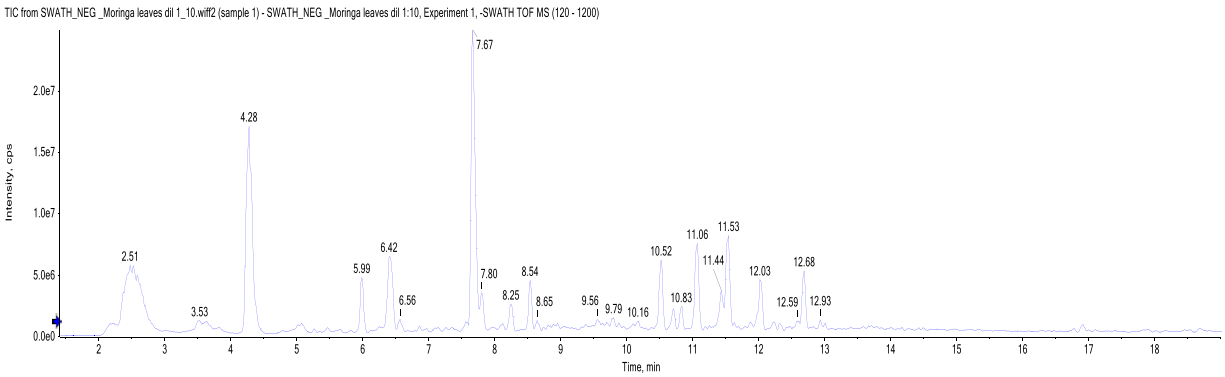

Fig. 1. Total ion current of Moringa leaves extract.

Glucose lactate and free fatty acid culture media levels

The cell culture media glucose and lactate levels were determined spectrophotometrically by a manual procedure using a commercial test kit (Greiner Diagnostic GmbH, Bahlingen-Germany) as previously described (Sabatini et al., 2011).

The cell culture media free fatty acid levels were determined spectrophotometrically by a manual procedure using a commercial test kit (Sigma-Aldrich, St. Louis, MO, USA). Briefly, 50 μl medium were incubated in a Acyl-CoA-Synthetase-Oxidase-Peroxidase buffer, and after incubation spectrophotometrically read at 570 nm. Samples OD were compared according to manufacturer recommendations, to those obtained by using Palmitic acid standards. FFAs amounts are presented as the increase relative to control cells.

Enzymatic activities

After each treatment, cells were trypsinized and centrifuged at 1200 × g for 10 minutes at room temperature. Cells were then lysed and the obtained supernatants were tested for protein content using the Bradford method (Sigma-Aldrich). Lactate dehydrogenase (LDH), citrate synthase (CS), 3-hydroxy acylCoA dehydrogenase (HAD) and alanine transglutaminase (ALT) enzymatic activities were then analyzed spectrophotometrically (Perkin Elmer Lambda 25, Fremont, CA, USA) as previously described (Duranti et al., 2011).

Creatine kinase (CK) activity measurements were performed by a manual procedure according to the manufacturer's recommendations in a hexokinase-glucose 6 phosphate-G6P dehydrogenase buffer assay using a commercial test kit (Greiner Diagnostic GmbH, Bahlingen–Germany) (Magi et al., 2018).

Preparation of cell homogenates and western blot analysis

Following the indicated treatment, samples were divided for cellular and mitochondrial extracts as previously described (Duranti et al., 2011). The extracted proteins were used immediately or divided and stored at -80°C until used.

Cellular proteins (10–20 μg in 25 mM Tris-HCl pH 8, 0.5% SDS, 0.05% 2-mercaptoethanol, 2.5% glycerol, and 0.001% bromophenol blue) were denatured at 100°C for 5 minutes, subjected to SDS-PAGE in a 8–12% polyacrylamide gel, and then electroblotted onto a PVDF membrane at 130 V for 1 hour. The blots were blocked with 5% non-fat dry milk (Bio-Rad Laboratories, Inc. Hercules, CA, USA) and then incubated with anti-SIRT1, anti-PPARα or anti-GLUT4 antibodies (Santa Cruz Biotechnology, Santa Cruz, CA, USA). After washing and incubation with a horseradish peroxidase–conjugated secondary antibody, the blots were developed with ECL (Amersham Biosciences, GE Healthcare Europe GmbH, Glattbrugg, Switzerland). Bands were quantified using ImageJ software (Rasband, W.S., ImageJ, U. S. National Institutes of Health, Bethesda, Maryland, USA, http:// rsb.info.nih.gov/ij, 1997–2008). The expression of β-actin (Sigma-Aldrich, St. Louis, MO) or COXIV (Santa Cruz Biotechnology, Santa Cruz, CA, USA) was used to normalise the data.

Statistical analysis

The Kolmogorov-Smirnov test was used to evaluate the variable distribution.

All data are expressed as means ± S.D. of three independent experiments, each performed in triplicate.

A one-way ANOVA for repeated measures and Bonferroni post-hoc analyses were used to determine significant variations over time and among groups for each parameter evaluated. $P<0.05$ was accepted as significant. The SPSS statistical package (Version 17.0 for Windows; SPSS Inc., Chicago, IL, USA) was used for statistical analysis.

No statistical differences were found in all parameters analyzed between untreated controls at T0, T24 and T48 hours (data not shown).

Results

Metabolomic fingerprint by UHPLC QTOF

The metabolomic profile on MOLE, was carried out by using the X500R QTOF mass spectrometer. To get the digital fingerprint and avoid any loss of information about the sample, a Data Independent Acquisition (SWATH) method was developed. SWATH acquisition has the primary advantage to allow the collection of MS/MS spectral information for every detectable precursor in the defined mass range. This allows product ion spectral information to be searched in a database for potential compound identification. For this purpose, the SCIEX Natural Products Library 2.0 was used to get high confidence in the identification of the main compounds (library match score >75% and mass error +/-2 ppm). The obtained profile is shown in Fig. 1 and highlighted the presence of glucosinolates, flavonoids and phenolic acids as already reported for this specie (Maldini M. et al, 2014). The proposed identification for flavonoids, polyphenols and phenolic acids is listed in the Table 1.

The most intense peaks are represented by glucosinolates (GS), that structurally are thioglucoside compounds, containing a sulfated aldoxime moiety and a variable side chain derived from amino acids. These metabolites are widely distributed in Brassicaceae family and in Moringa plant and well known for their important biological activities in particular the anti-carcinogenic and antioxidant effects (Maldini M et al, 2012).

Due to the lack of reference compounds, their putative identification was performed manually, considering their diagnostic and characteristic fragments at m/z values of 259.01 and 96.96 which can be assigned to the sulfated glucose moiety and the sulfate group, respectively (Bennett et al., 2003; Fahey et al., 2018). The Fig. 2 reports the eXtracted Ion Chromatogram obtained for typical glucosinolates: Glucomoringin (a), 4-O-acetylrhamnopyranosyloxybenzylGS and its isomers

Table 1
Proposed identification for flavonoids, polyphenols and phenolics acids reported with formula, exact mass, main diagnostic fragments in high resolution and library score.

Proposed Identification	Retention Time	Adduct / Charge	Formula	Precursor Mass	Mass Error (ppm)	MSMS	Library Score
Quinic acid	2.59	[M-H]-	C7H12O6	191.056	−1	85.0291	78
Citric acid	3.34	[M-H]-	C6H8O7	191.02	0.2	111.006	97
Neochlorogenic acid	6.26	[M-H]-	C16H18O9	353.088	−2.3	191.0613	97.9
Chlorogenic acid	6.44	[M-H]-	C16H18O9	353.088	−2.3	191.0534	97.9
Protocatechuic acid	6.5	[M-H]-	C7H6O4	153.019	0.8	109.0292	84.3
Esculin	7.15	[M-H]-	C15H16O9	339.072	−0.8	177.0196	97.3
Cryptochlorogenic acid	7.8	[M-H]-	C16H18O9	353.088	−2.3	135.0435	97.9
Vitamin B2	8.74	[M-H]-	C17H20N4O6	375.131	−0.6	255.0894	97.4
Quercetin-di-O-glucoside	9.36	[M-H]-	C27H30O17	625.142	0	463.0893	94.7
Orientin	9.64	[M-H]-	C21H20O11	447.093	−0.7	327.0511	100
Rutin	10.52	[M-H]-	C27H30O16	609.146	−1.9	301.0313	96.7
Vitexin	10.71	[M-H]-	C21H20O10	431.098	−2.4	311.0534	98.1
Isovitexin	10.83	[M-H]-	C21H20O10	431.098	−2.4	341.0637	98.1
Isoquercitrin	11.06	[M-H]-	C21H20O12	463.088	−3	300.024	99.5
Kaempferol-O-rutinoside	11.44	[M-H]-	C27H30O15	593.151	−2.1	285.0369	97.5
Quercetin-O-β-D-glucose-acetate isomer	11.53	[M-H]-	C23H22O13	505.098	−1	300.0251	97.7
Isorhamnetin-O-neohespeidoside	11.64	[M-H]-	C28H32O16	623.162	−0.3	315.0507	94
Quercetin-O-β−D-glucose-acetate isomer	11.98	[M-H]-	C23H22O13	505.098	−1	300.0251	96
Astragalin/Luteoloside	12.03	[M-H]-	C21H20O11	447.093	−1.5	284.0296	100
Nepetin 7-glucoside	12.24	[M-H]-	C22H22O12	477.103	−0.9	315.0486	82
Puerarin	12.25	[M-H]-	C21H20O9	415.103	1.2	295.0613	96.1
Quercetin-O-β-D-glucose-acetate isomer	12.34	[M-H]-	C23H22O13	505.098	−0.9	300.0251	98.3
Ferulic/Isoferulic acid	13.67	[M-H]-	C10H10O4	193.051	0.4	134.037	97.2
Kaempferol 3-O-(3″,4″-di-O-acetyl-α-L-rhamnopyranoside)	14.98	[M-H]-	C25H24O12	515.119	−0.5	284.0327	100
Quercetin	15.36	[M-H]-	C15H10O7	301.035	−0.8	151.0032	96.6
Kaempferol	17.52	[M-H]-	C15H10O6	285.04	−0.4		63.6
Isorhamnetin	17.88	[M-H]-	C16H12O7	315.051	1	300.0281	87.9

Table 2
Proposed identification for glucosinolates.

Proposed identification	Retention Time	Adduct / Charge	Precursor Mass	Mass Error (ppm)	Fragment Mass	Fragment Mass Error (ppm)
Sinalbin	4.28	[M-H]-	424.0381	0.9	96.9601	−0.2
Glucosoonjnain	3.81	[M-H]-	586.0902	−0.2	96.9596	−7.4
Glucomoringin (a)	4.28	[M-H]-	570.0916	0.2	96.9579	1.1
					259.0107	1.6
4-O-acetylrhamnopyranosyloxybenzyl-GS/5.99 (b)	5.99	[M-H]-	612.1028	−0.3	96.958	−1.2
					259.0122	0
4-O-acetylrhamnopyranosylosxybenzyl-GS/6.41 (c)	6.4	[M-H]	612.1039	−0.1	96.9586	0
					259.013	0.1
4-O-acetylrhamnopyranosyloxybenzyl-GS/7.67 (d)	7.68	[M-H]	612.1018	−0.3	96.9584	−5
					259.0102	−2.4
4-O-acetylglucopyranosyloxybenzyl-GS/6.97 (e)	6.98	[M-H]	628.099	−0.8	96.9593	−4.3
					259.0129	0
4-O-acetylglucopyranosyloxybenzyl-GS/5.34	5.33	[M-H]	628.1012	−1.3	96.9597	−2.8

(b-d), 4-O-acetylglucopyranosyloxybenzylGS (e). Each glucosinolates is extracted considering the diagnostic fragments as listed in the Table 2, where are reported all found glucosinolates.

Fig. 3 shows the amount of each components represented by chromatographic peak area.

Antioxidant capacity of MOLE

Different diluton of the methanolic extract of *Moringa oleifera* leaves stock solution were tested for antioxidant capacity. The Trolox® equivalent antioxidant capacity of MOLE was determined. Results are shown in Fig. 4. Dilutions of MOLE extract were linear up to 1/100 working solution. 1/1000 and 1/100 working solution were selected for cells treatment.

Effect of MOLE on glucose, free fatty acids and lactate levels and GLUT4 protein level

Substrate consumption was evaluated by analyzing culture medium glucose, lactate and FFA levels. No differences were found in controls with or without vehicle (Table 3). MOLE exposure induced a time and dose-dependent decrease in glucose and FFAs and an increase in lactate levels in culture medium compared to control (Table 3).

When compared to control methanol (CTRLm), MOLE decreased glucose (11.4 ± 1.3 and 19.2 ± 2.9 % for MOLE 1/1000 and 1/100 respectively after 24 h treatment, $p<0.05$, and 16.7 ± 2.9 and 28.2 ± 2.4 % for MOLE 1/1000 and 1/100 respectively after 48 h treatment, $p<0.05$) and FFA (13.7 ± 5.1 and 24.2 ± 5.0 % for MOLE 1/1000 and 1/100 respectively after 24 h treatment, $p<0.05$, and 31.1 ± 2.0 and 50.8 ± 3.5 % for MOLE 1/1000 and 1/100 respectively after 48 h treatment, $p<0.05$) levels in culture medium (Fig. 5). Moreover MOLE induced lactate release (5.0 ± 0.9 and 11.4 ± 0.6 % for MOLE 1/1000 and 1/100 respectively after 24 h treatment, $p<0.05$, and 7.9 ± 2.5 and 13.8 ± 3.9 % for MOLE 1/1000 and 1/100 respectively after 48 h treatment, $p<0.05$) (Fig. 5).

MOLE treatment induced a slight but not statistically significant ($p=0.5$) increase in GLUT4 protein levels compared to control myotubes. No dose or time dependent effect was found (Fig. 5).

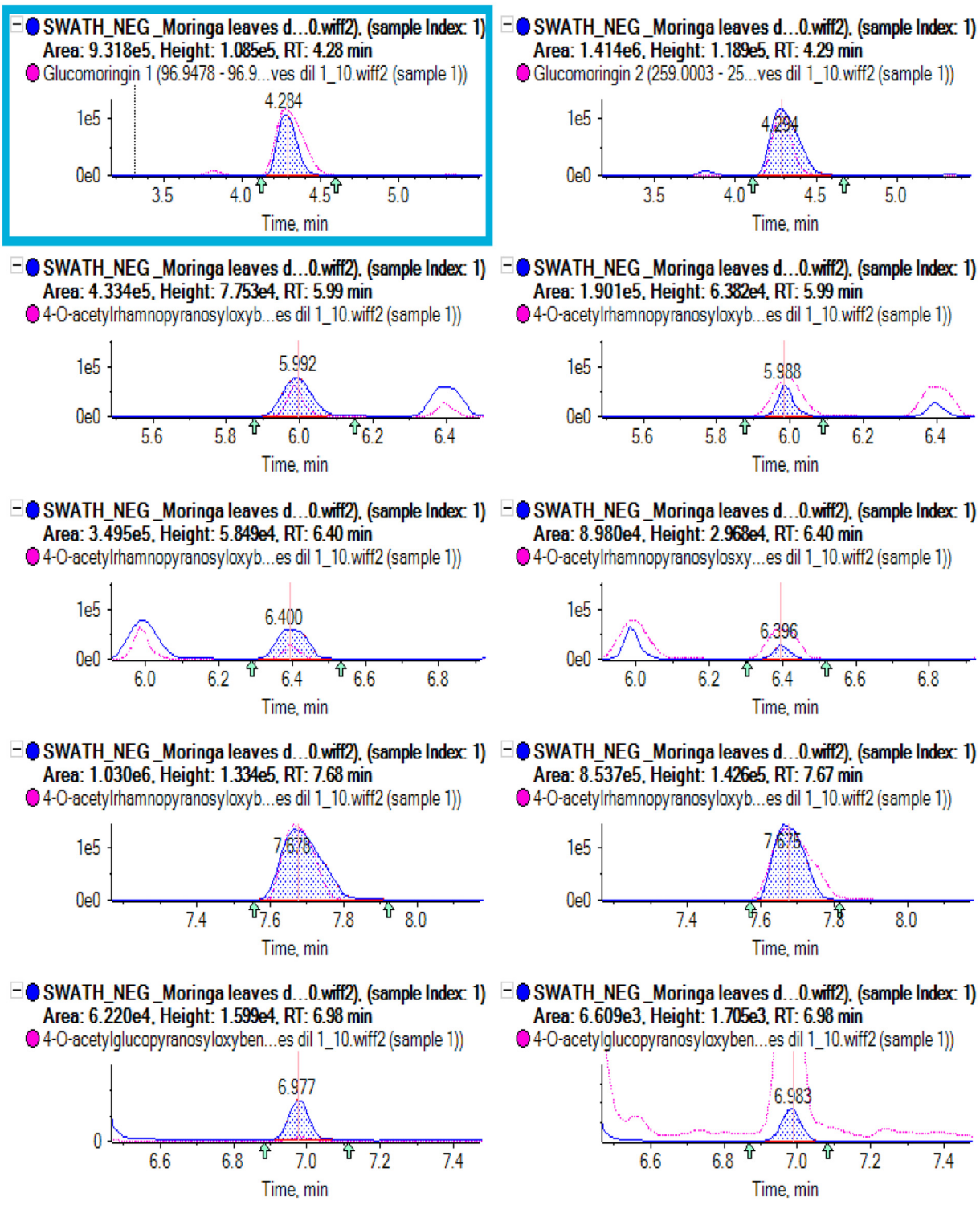

Fig. 2. Extracted ion chromatogram in UHPLC TOF SWATH MSMS.

Effect of MOLE on C2C12 myotubes CS, LDH, HAD, ALT, CK activity levels

C2C12 metabolism was evaluated by analyzing CS, LDH, HAD, ALT, CK enzyme activity levels. No differences were found in controls with or without vehicle (Table 4). MOLE exposure induced an increase in citrate synthase, 3-hydroxy acylCoA dehydrogenase and creatine kinase activity levels compared to control in a time and dose independent manner (Table 4). Alanine transglutaminase and lactate dehydrogenase activities increased only after 48 hours MOLE 1/1000 treatment compared to controls. No differences were found between MOLE 1/1000 and 1/100.

When compared to control methanol (CTRLm), MOLE induced an increase in CS activity after 24 hours treatment (27.3 ± 14.0 and 42.5 ± 13.0 % for MOLE 1/1000 and 1/100 respectively, $p<0.05$) and after 48 hours treatment (30.9 ± 17.3 and 30.3 ± 11.1 % for MOLE 1/1000 and 1/10, $p<0.05$).

Table 3
Culture media substrate levels.

	24 hours					48 hours				
	CTRL	CTRLm	MOLE 1/1000	MOLE 1/100	I	CTRL	CTRLm	MOLE 1/1000	MOLE 1/100	I
GLU (mM/L)	20.39 ± 0.73	19.97 ± 0.37	17.69 ± 0.23 * #	16.13 ± 0.35 * #	14.26 ± 0.61 * #	11.99 ± 0.62	11.45 ± 0.62	9.55 ± 0.82 * #	8.23 ± 0.70 * #	7.85 ± 0.25 * #
FFAs (μM/L)	23.41 ± 1.14	23.67 ± 0.63	20.41 ± 0.67 * #	17.92 ± 0.71 * #	17.78 ± 0.62 * #	12.18 ± 2.57	13.32 ± 2.02	9.19 ± 1.59 #	6.60 ± 1.42 * #	7.06 ± 0.99 * #
LAC (mM/L)	8.73 ± 0.48	8.99 ± 0.21	9.44 ± 0.15 #	10.02 ± 0.18 * #	10.09 ± 0.17	10.60 ± 0.79	11.16 ± 0.79	12.02 ± 0.58 *	12.69 ± 0.66	12.30 ± 0.79

GLU, glucose; FFAs, free fatty acids; LAC, lactate; CTRL, control; CTRLm, control methanol; I, insulin. Myotubes were treated with MOLE stock solution diluitions (1/1000 and 1/100 working solutions) or methanol (CTRLm) for 24 and 48 hours and culture media was immediately tested for biochemical parameters. Data are expressed as mean ± S.D. of three independent experiments, each performed in triplicate. *p<0.05 vs. respective CTRL; #p<0.05 vs. respective CTRLm.

Table 4
C2C12 myotubes enzymatic activities.

	24 hours				48 hours			
	CTRL	CTRLm	MOLE 1/1000	MOLE 1/100	CTRL	CTRLm	MOLE 1/1000	MOLE 1/100
CS (mU/mg)	98.71 ± 6.26	102.84 ± 5.81	130.42 ± 8.18 * #	146.14 ± 7.30 * #	121.34 ± 6.35	133.13 ± 10.13	173.15 ± 8.67 * #	172.84 ± 6.51 * #
HAD (mU/mg)	28.39 ± 0.49	29.95 ± 1.81	35.57 ± 1.76 * #	37.08 ± 2.18 * #	36.59 ± 2.50	38.03 ± 0.90	45.61 ± 1.66 * #	48.83 ± 2.26 * #
LDH (U/mg)	29.07 ± 1.98	34.12 ± 3.47	31.68 ± 3.70	26.77 ± 1.36 #	32.45 ± 4.12	36.22 ± 5.15	35.45 ± 2.54	28.81 ± 2.60
ALT (U/mg)	3.88 ± 0.09	4.02 ± 0.05	4.09 ± 0.06 *	4.16 ± 0.07 * #	4.14 ± 0.10	4.27 ± 0.02	4.45 ± 0.09 * #	4.59 ± 0.04 * #
CK (U/g)	1.96 ± 0.01	1.96 ± 0.01	1.98 ± 0.01 * #	2.15 ± 0.04 * #	2.08 ± 0.02	2.10 ± 0.02	2.28 ± 0.10 * #	2.51 ± 0.06 * #

CSH, citrate synthase; HAD, 3-hydroxy acylCoA dehydrogenase; LDH, lactate dehydrogenase; ALT, alanine transglutaminase; CK, creatine kinase; CTRL, control; CTRLm, control methanol. Myotubes were treated with MOLE stock solution diluitions (1/1000 and 1/100 working solutions) or methanol (CTRLm) for 24 and 48 hours and cells extracts were tested for biochemical analysis. Data are expressed as mean ± S.D. of U enzyme/mg protein of three independent experiments, each performed in triplicate. *p<0.05 vs. respective CTRL; #p<0.05 vs. respective CTRLm.

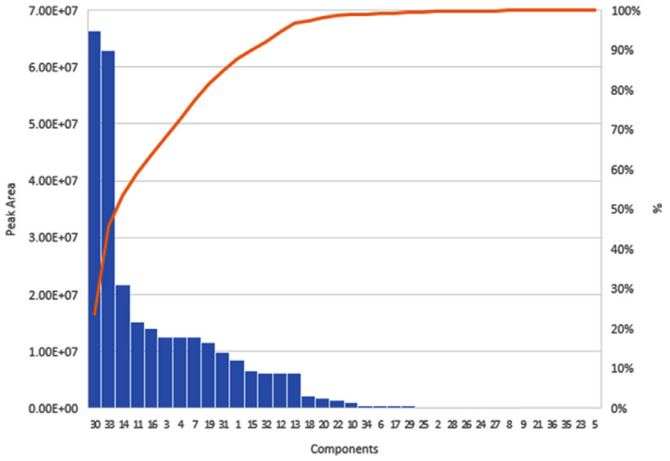

Fig. 3. Relative amounts of components in Moringa samples
1) Quinic acid; 2) Citric acid; 3) Neochlorogenic acid; 4) Chlorogenic acid; 5) Protocatechuic acid; 6) Esculin; 7) Cryptochlorogenic acid; 8) Vitamin B2; 9) Quercetin-di-O-glucoside; 10) Orientin; 11) Rutin; 12) Vitexin; 13) Isovitexin; 14) Isoquercitrin; 15) Kaempferol-rutinoside; 16) Quercetin-O-glucose-acetate isomer; 17) Isorhamnetin-neohespeidoside; 18) Quercetin-O-glucose acetate isomer; 19) Astragalin/Luteoloside; 20) Nepetin 7-glucoside; 21) Puerarin; 22) Quercetin-O- glucose-acetate isomer; 23) Ferulic/Isoferulic acid; 24) Kaempferol 3-O-(3″,4″-di-O-acetyl-a-L-rhamnopyranoside); 25) Quercetin; 26) Kaempferol; 27) Isorhamnetin; 28) Sinalbin; 29) Glucosoonjnain; 30) Glucomoringin; 31) 4-O-acetylrhamnopyranosyloxybenzylGS/5.99; 32) 4-O-acetylrhamnopyranosylosxybenzylGS/6.41; 33) 4-O-acetylrhamnopyranosyloxybenzylGS/7.67; 34) 4-O-acetylglucopyranosyloxybenzylGS/6.97; 35) 4-O-acetylglucopyranosyloxybenzylGS/6.16; 36) 4-O-acetylglucopyranosyloxybenzylGS/5.34

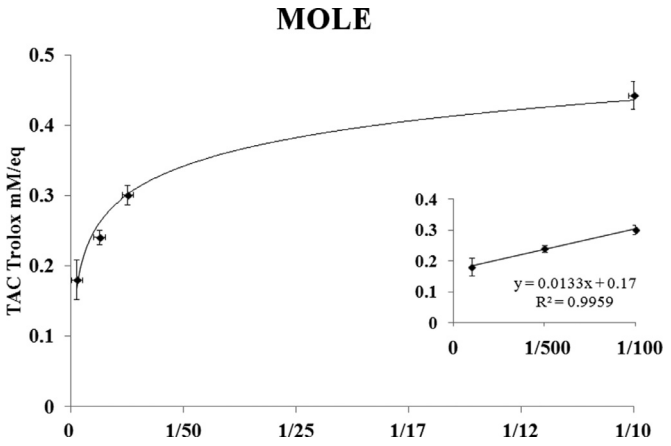

Fig. 4. MOLE in vitro modified Trolox® equivalent antioxidant capacity assay. MOLE stock solution dilutions (1/1000–1/500–1/100 and 1/10 working solution) were tested and the variation of absorbance ΔOD/min734 was recorded and compared to those obtained using Trolox® standards.

HAD activity increased after 24 hours treatment (18.8 ± 1.7 and 23.9 ± 4.2 % for MOLE 1/1000 and 1/100 respectively p<0.05) and after 48 hours treatment (20.0 ± 7.0 and 28.3 ± 2.9 % for MOLE 1/1000 and 1/100 respectively, p<0.05).

CK activity was increased after 24 hours treatment (1.6 ± 0.9 and 9.2 ± 2.5 % for MOLE 1/1000 and 1/100 respectively, p<0.05) and after 48 hours treatment (8.7 ± 3.8 and 20.0 ± 2.2 % for MOLE 1/1000 and 1/100 respectively, p<0.05) (Fig. 6).

MOLE 1/100 treatment induced an increase in ALT (7.46 ± 0.3 %, p<0.05) and a decrease in LDH (23.47 ± 11.8 %, p<0.05) activities after 48 hours treatment (Fig. 6).

Effect of MOLE on C2C12 myotubes SIRT1 and PPARα protein levels

MOLE exposure was able to increase SIRT1 and PPARα protein content after 24 and 48 hours of treatment compared to control, with no significant dose or time dependent effect (Fig. 7). Total mitochondrial protein amount was also increased by MOLE treatment (p<0.05), however no significant dose or time dependent effects were found (p>0.05, Fig. 7).

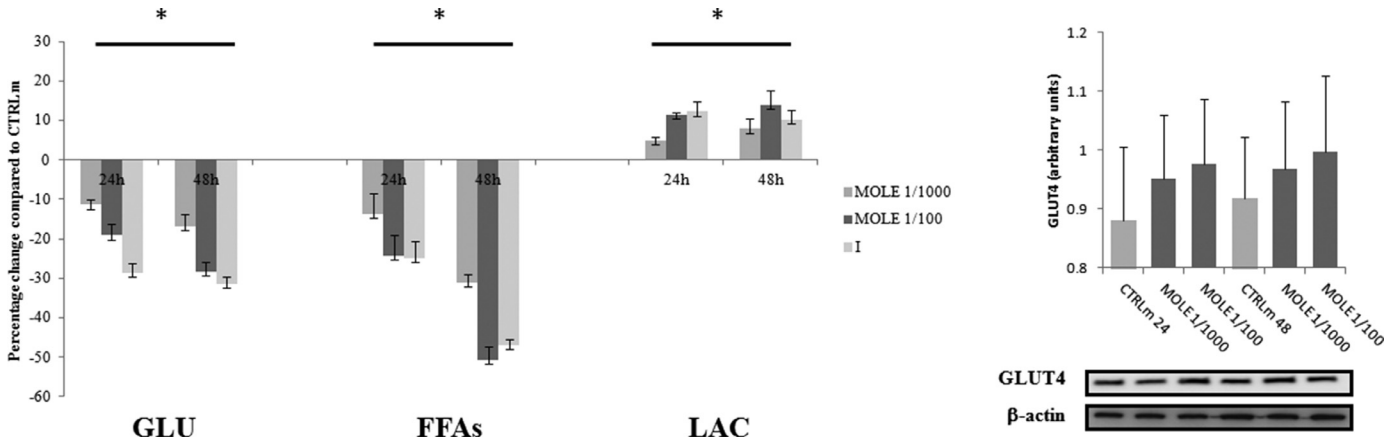

Fig. 5. Glucose (GLU), free fatty acid (FFAs) and lactate (LAC) culture media levels and GLUT4 protein level after MOLE treatment.
C2C12 myotubes were treated for 24 and 48 h with MOLE at 1/1000 and 1/100 working solutions or insulin (I) 100 nM. Glu, FFA and lactate culture media levels were then measured. The histograms represent the mean ± S.D. percentage change compared to respective CTRLm. *p<0.05 compared to CTRLm. GLUT4 protein expression was measured and expressed as the ratio between the optical density (OD) of the marker protein and the OD of *β*-actin. Images show representative immunoblotting results. The histograms represent the mean ± S.D. *p<0.05 compared to CTRLm.

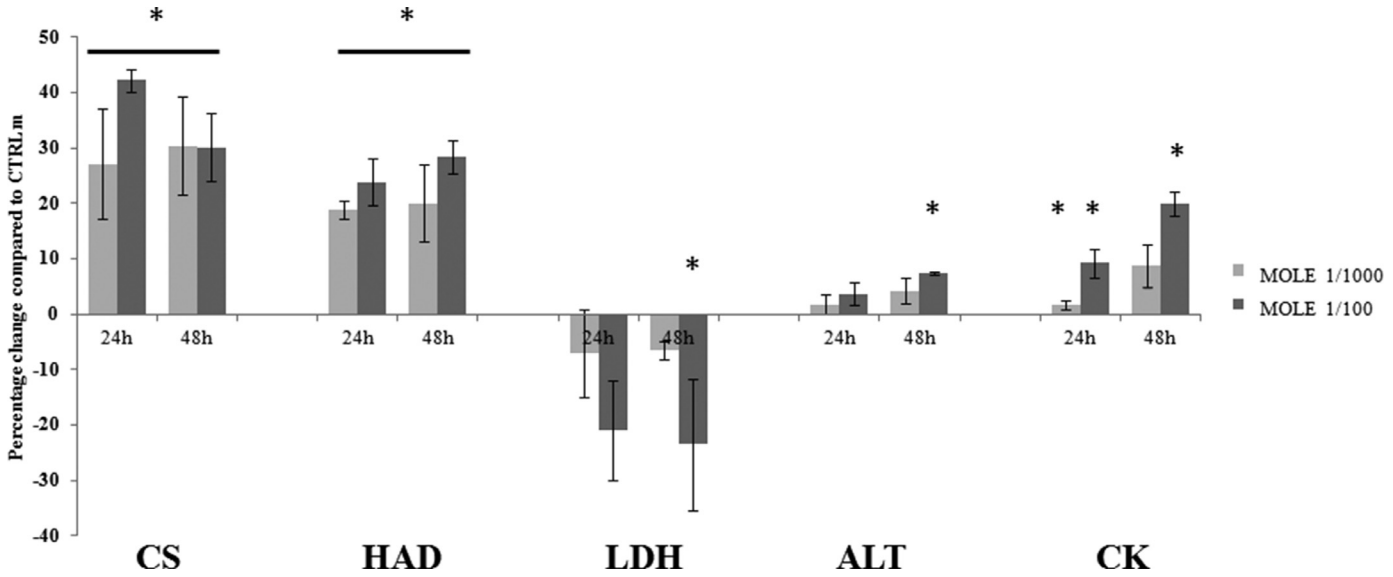

Fig. 6. C2C12 myotubes CS, HAD, LDH, ALT and CK activity levels percentage change after MOLE treatment.
C2C12 myotubes were treated for 24 and 48 h with MOLE at 1/1000 and 1/100 working solutions. Cellular citrate synthase (CS), 3-hydroxy acylCoA dehydrogenase (HAD), lactate dehydrogenase (LDH), alanine transglutaminase (ALT). and creatine kinase (CK) activity levels were then measured. The histograms represent the mean ± S.D. percentage change compared to respective CTRLm. *p<0.05 compared to CTRLm.

Discussion

In this study, we demonstrate that *Moringa oleifera* leaf extract is able to increase energy metabolism in muscle cells. After MOLE treatment, a dose and time dependent increase in culture medium substrate consumption and an increase of intracellular metabolism enzyme activities were observed in C2C12 myotubes. Regarding the molecular mechanism, the MOLE treatment modulated positively the protein expression of SIRT1 and PPAR*α*.

Skeletal muscle represents the largest insulin-sensitive tissue in the human body and it acts a primary site of insulin resistance in the context of metabolic disease (Bouzakri et al., 2005). Stimulation of muscle FA oxidation by preventing FA accumulation and peroxidation has emerged as a strategy for the treatment of insulin resistance (Kiens et al., 2011). In this context, the use of nutritional strategies capable of optimizing the use of substrates and activating mitochondrial biogenesis may be useful in counteracting skeletal muscle stress in physiopathological conditions.

Many studies have proved that MOLE extract has antihyperglycemic and hypoglycemic activity in rats, effects which might be mediated through the stimulation of insulin release leading to enhanced glucose uptake and glycogen synthesis (Nova et al., 2020).

Here, we found that glucose culture medium decreased dose and time-dependently indicating increased substrate consumption in the treated myotubes. MOLE treatment did not influence gene expression in fact GLUT4 protein levels were not affected by treatment. However, it must be taken into consideration, that we did not determine the cellular localization of GLUT4 but only the total protein content and therefore it cannot be ruled out that a greater translocation of the transporter occurred following MOLE treatment.

Interestingly in our experimental model, MOLE treatment was able to reduce culture medium FFAs in a dose and time-dependent manner. Usually FFAs consumption is followed by an increased oxidative metabolism and mitochondrial content.

Indeed, we found that MOLE increased the level of mitochondrial proteins in a dose and time-dependent manner. To investigate the mech-

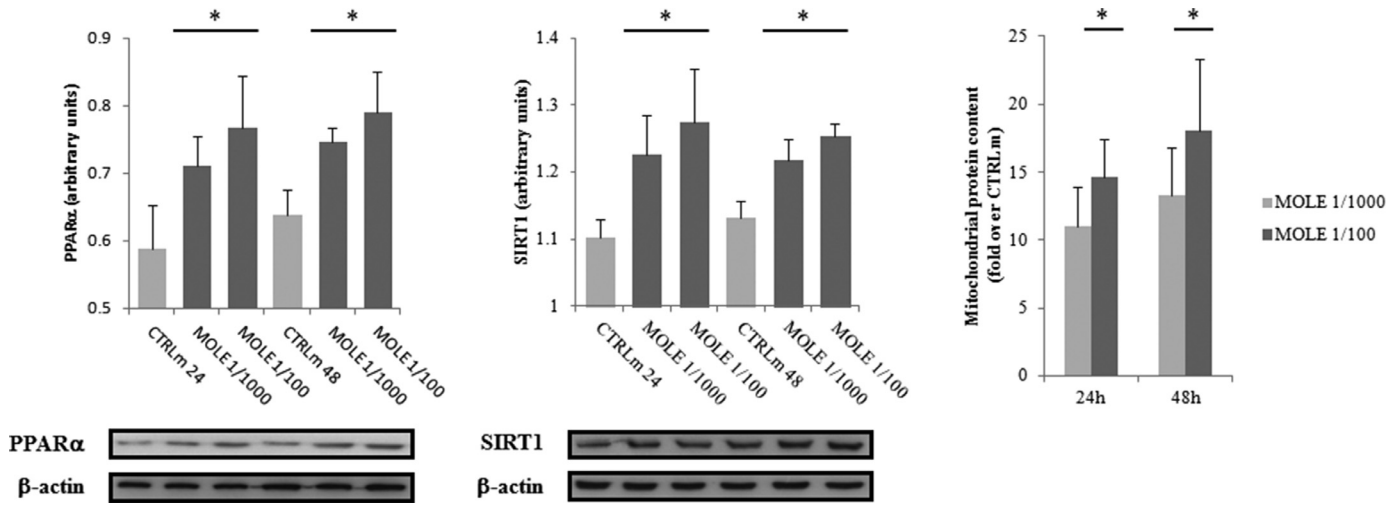

Fig. 7. Modulation of SIRT1 and PPARα protein levels and mitochondrial protein content after MOLE treatment in C2C12 myotubes.
C2C12 myotubes were treated for 24 and 48 h with MOLE at 1/1000 and 1/100 working solutions. Protein expression was then measured and expressed as the ratio between the optical density (OD) of the marker protein and the OD of β-actin. Images show representative immunoblotting results. The histograms represent the mean ± S.D. *p<0.05 compared to CTRLm.

anism by which MOLE exerts its effects, SIRT1and PPARα protein levels were analyzed.

SIRT1 is a key molecule in metabolic regulation and plays its role through its ability to deacetylate and activate PGC1α, a transcription co-regulator of PPARs (Pardo and Boriek, 2011), with the final result of increasing mitochondrial biogenesis and oxidative metabolism (Wu et al., 1999; Ferrè, 2004; Gurd, 2011). Among these receptors, PPARα is active in tissues with high levels of fatty acid oxidation such as skeletal muscle, cardiac muscle, liver, and the kidneys.

PPARα is activated transcriptionally by PGC1α thus regulating genes involved in lipid and glucose metabolism, adipocyte differentiation, fatty acid transport, and inflammation (Petr et al., 2018). PPARα has been suggested as an important therapeutic target for metabolic diseases with hyperlipidemia (Seok and Cha, 2013).

We found that, when compared to controls, MOLE treatment increased in a statistically significant manner SIRT1 and PPARα protein levels.

As a consequence of this pathway activation, citrate synthase and 3-hydroxy acyl-CoA dehydrogenase, key enzymes of oxidative metabolism were also increased.

Skeletal muscle is a uniquely plastic tissue and it adapts in response to physiological stimuli such as physical exercise. The adaptive response to an aerobic exercise, at biochemical level, includes the increase in number of mitochondria and oxidative metabolism enzymatic activities and therefore an increased capacity of the muscle to sustain aerobic metabolism (Holloszy and Coyle, 1984). Usually these events, leads also to an enhanced muscle mass, associated with an increased creatine kinase (CK) activity (Watchko et al., 1996; Zanou and Gailly, 2013).

Creatine kinase represents a reservoir of high-energy phosphates and plays a primary role in the maintenance of ATP homeostasis (Sahlin and Harris, 2011) related to the energetic demands of the muscle contractile proteins (Watchko et al., 1996). Here, we show that MOLE was able to increase CK activity in a dose and time-dependent manner.

It is well recognised that an active lifestyle benefits both the body and the brain but sometimes, due to injury, disease, or aging, people may not be able to exercise regularly so molecules that to some extent, mimic systemic and central effects of exercise could be a useful aid. Based on our results, it is possible to hypothesize that *Moringa oleifera* could be used as a nutritional exercise alternative.

Interestingly, a recent study reported that the *Moringa oleifera* leaf aqueous extract showed antifatigue properties, and improved the swimming performance of rats, probably by increasing the mobilization and use of body fats, and by slowing down the depletion of glycogen stores (Lamou et al., 2016).

In order to identify the bioactive molecules potentially responsible for MOLE biological effect, we screened the extract for phytochemicals determination.

In the current study, the metabolomic fingerprint obtained by UHPLC QTOF analysis highlighted the presence of glucosinolates (GS), flavonoids and phenolic acids. This is in accordance with our previous report for this specie (Maldini M. et al, 2014). The most intense peaks are represented by GS. These metabolites are widely distributed in Brassicaceae family and in Moringa plant and well known for their important biological activities in particular the anti-carcinogenic and antioxidant effects (Maldini M et al, 2012).

Moreover, among the biomolecules present in the MOLE extract, flavonoids and phenolics compounds due to their anti-inflammatory and antioxidant properties may be good candidates to validate the beneficial effects of MOLE on cell metabolism (Olayaki et al., 2015; Khan et al., 2017; Nova et al., 2020).

Among the bioactive compounds of MOLE, quercetin and glucomoringin showed anti-diabetic activity in animal models (Bhattacharya et al., 2018). Quercetin also showed the ability to promote mitochondrial biogenesis in skeletal muscles and therefore to augment mitochondrial training adaptations and/or mitochondrial protein content, enzyme activities, and/or respiratory function (Islam et al., 2020). We have recently demonstrated that acute and chronic quercetin supplementation were able to support physical exercise in young men (Patrizio et al., 2018; Bazzucchi et al., 2020).

As expected, the predominant glucosinolate found in MOLE is 4-(α-L-rhamnopyranosiloxy)benzyl glucosinolate, known as glucomoringin. This compound exhibits different biological properties distinctly different from those of others GS (Brunelli et al., 2010). Moreover, glicosinolates may induce metabolic changes rebalancing anaplerotic and cataplerotic reactions and restoring metabolic homeostasis (Armah et al., 2013). The role in regulation of metabolism and optimization of substrates could explain the beneficial feature of the consumption of vegetables rich in isothiocyanates and glucosinolates on the prevention of different pathologies such as cancer.

However, it must be considered that the combination of micronutrients such as that which is present in *Moringa oleifera* leaf extract is probably more effective than the administration of a single molecule

considering that some micronutrients may have mutually beneficial or synergical effects on muscle health.

Conclusions

Optimising oxidative metabolism by dietary strategies may be useful in counteracting skeletal muscle stress in physiopathological conditions.

Our data indicate that MOLE is able to increase myotubes oxidative metabolism and therefore could represent an important nutritional support for people unable to perform regular physical activity.

While the aim of this work was to evaluate the biological effect of MOLE per se, it should be acknowledged that further studies are needed to analyze the biological effects of the single compounds highly represented in the extract. This could be fundamental in assisting to clarify the exercise-mimetic effect of MOLE.

Authors contributions

Guglielmo Duranti: Conceptualization, Investigation, Methodology, Writing original draft, Writing, review & editing.

Maldini Mariateresa: Writing, review & editing.

Domenico Crognale: Software, Writing original draft, Writing, review & editing.

Stefania Sabatini: Conceptualization, Supervision, Writing, review & editing.

Corana Federica: Writing, review & editing.

Katy Horner: Conceptualization, Supervision, Writing original draft, Writing, review & editing.

Roberta Ceci: Investigation, Methodology, Software, Writing original draft, Writing, review & editing.

All data were generated in-house, and no paper mill was used. All authors agree to be accounTable for all aspects of work ensuring integrity and accuracy.

Declaration of Competing Interest

The authors have no conflicts of interest to declare.

Acknowledgments

Funding: This research did not receive any specific grant from funding agencies in the public, commercial, or not-for-profit sectors.

We thank Prof. Fabio Virgili and Dr. Fausta Natella, [(CREA), Food and Nutrition Research Centre, Via Ardeatina 546, 00178 Roma, Italy] for their helpful support.

References

Armah, CN, Traka, MH, Dainty, JR, Defernez, M, Janssens, A, Leung, W, Doleman, JF, Potter, JF, Mithen, RF., 2013. A diet rich in high-glucoraphanin broccoli interacts with genotype to reduce discordance in plasma metabolite profiles by modulating mitochondrial function. Am. J. Clin. Nutr. 98 (3), 712–722. doi:10.3945/ajcn.113.065235.

Bais, S., Singh, G.S., Sharma, R., 2014. Anti obesity and hypolipidemic activity of Moringa Oleifera leaves against high fat diet induced obesity in rats. Adv. Biol. 1–9. doi:10.1155/2014/162914.

Bazzucchi, I., Patrizio, F., Ceci, R., Duranti, G., Sabatini, S., Sgrò, P., Di Luigi, L., Sacchetti, M., 2020. Quercetin supplementation improves neuromuscular function recovery from muscle damage. Nutrients 12, 2850. doi:10.3390/nu12092850.

Bennett, R.N., Mellon, F.A., Foidl, N., Pratt, J.H., Dupont, M.S., Perkins, L., Kroon, P.A., 2003. Profiling glucosinolates and phenolics in vegetative and reproductive tissues of the multi-purpose trees Moringa oleifera L. (horseradish tree) and Moringa stenopetala L. J. Agric. Food Chem. 51 (12), 3546–3553. doi:10.1021/jf0211480, 4.

Bhattacharya, A., Tiwari, P., Sahu, P.K., Kumar, S., 2018. A review of the phytochemical and pharmacological characteristics of Moringa Oleifera. J. Pharm. Bioallied. Sci. 10 (4), 181–191. doi:10.4103/JPBS.JPBS_126_18.

Bouzakri, K., Koistinen, H.A., Zierath, J.R., 2005. Molecular mechanisms of skeletal muscle insulin resistance in type 2 diabetes. Curr. Diabetes Rev. 1 (2), 167–174. doi:10.2174/1573399054022785.

Brunelli, D., Tavecchio, M., Falcioni, C., Frapolli, R., Erba, E., Iori, R., Rollin, P., Barillari, J., Manzotti, C., Morazzoni, P., D'Incalci, M, 2010. The isothiocyanate produced from glucomoringin inhibits NF-kB and reduces myeloma growth in nude mice in vivo. Biochem. Pharmacol. 79, 1141.

De Fronzo, R.A., Tripathy, D., 2009. Skeletal muscle insulin resistance is the primary defect in type 2 diabetes. Diabetes Care. 32, S157–S163. doi:10.2337/dc09-S302.

Duranti, G., La Rosa, P., Dimauro, I., Wannenes, F., Bonini, S., Sabatini, S., Parisi, P., Caporossi, D., 2011. Effects of salmeterol on skeletal muscle cells: metabolic and proapoptotic features. Med. Sci. Sports Exer. 43 (12), 2259–2273. doi:10.1249/MSS.0b013e3182223094.

Duranti, G., Ceci, R., Sgrò, P., Sabatini, S., Di Luigi, L., 2017. Influence of the PDE5 inhibitor tadalafil on redox status and antioxidant defense system in C2C12 skeletal muscle cells. Cell Stress Chaperones 22 (3), 389–396. doi:10.1007/s12192-017-0778-9.

Fahey, J.W., Olson, M.E., Stephenson, K.K., Wade, K.L., Chodur, G.M., Odee, D., Nouman, W., Massiah, M., Alt, J., Egner, P.A., Hubbard, W.C., 2018. The diversity of chemoprotective glucosinolates in moringaceae (Moringa spp. Sci. Rep. 8 (1), 7994. doi:10.1038/s41598-018-26058-4.

Ferrè, P., 2004. The biology of peroxisome proliferator-activated receptors: relationship with lipid metabolism and insulin sensitivity. Diabetes 53 (Suppl 1), S43–S50. doi:10.2337/diabetes.53.2007.s43.

Gurd, B.J., 2011. Deacetylation of PGC-1α by SIRT1: importance for skeletal muscle function and exercise-induced mitochondrial biogenesis. Appl. Physiol. Nutr. Metab. 36 (5), 589–597. doi:10.1139/h11-070.

Holloszy, J.O., Coyle, E.F., 1984. Adaptations of skeletal muscle to endurance exercise and their metabolic consequences. J. Appl. Physiol. Respir. Environ. Exerc. Physiol. 56 (4), 831–838. doi:10.1152/jappl.1984.56.4.831.

Khan, W, Parveen, R, Chester, K, Parveen, S, Ahmad, S., 2017. Hypoglycemic potential of aqueous extract of moringa oleifera leaf and In Vivo GC-MS metabolomics. Front. Pharmacol. 8, 577. doi:10.3389/fphar.2017.00577.

Kiens, B., Alsted, T.J., Jeppesen, J., 2011. Factors regulating fat oxidation in human skeletal muscle. Obes. Rev. 12 (10), 852–858. doi:10.1111/j.1467-789X.2011.00898.x.

Kou, X., Li, B., Olayanju, J.B., Drake, J.M., Chen, N., 2018. Nutraceutical or pharmacological potential of Moringa Oleifera Lam. Nutrients 10 (3), 343. doi:10.3390/nu10030343.

Islam, H., Hood, D.A., Gurd, B.J., 2020. Looking beyond PGC-1α: emerging regulators of exercise-induced skeletal muscle mitochondrial biogenesis and their activation by dietary compounds. Appl. Physiol. Nutr. Metab. 45 (1), 11–23. doi:10.1139/apnm-2019-0069.

Lamou, B., Taiwe, G.S., Hamadou, A., Abene Houlray, J., Atour, M.M., Tan, P.V, 2016. Antioxidant and antifatigue properties of the aqueous extract of moringa oleifera in rats subjected to forced swimming endurance test. Oxid. Med. Cell Longev. 2016, 3517824. doi:10.1155/2016/3517824.

Magi, F., Dimauro, I., Margheritini, F., Duranti, G., Mercatelli, N., Fantini, C., Ripani, F.R., Sabatini, S., Caporossi, D., 2018. Telomere length is independently associated with age, oxidative biomarkers, and sport training in skeletal muscle of healthy adult males. Free Radic. Res. 52 (6), 639–647. doi:10.1080/10715762.2018.1459043.

Maldini, M., Baima, S., Morelli, G., Scaccini, C., Natella, F., 2012. A liquid chromatography-mass spectrometry approach to study "glucosinoloma" in broccoli sprouts. J. Mass Spectrom. 47 (9), 1198–1206. doi:10.1002/jms.3028.

Maldini, M., Maksoud, S.A., Natella, F., Montoro, P., Petretto, G.L., Foddai, M., De Nicola, G.R., Chessa, M., Pintore, G., 2014. Moringa oleifera: study of phenolics and glucosinolates by mass spectrometry. J. Mass Spectrom. 49 (9). doi:10.1002/jms.3437, 900-10.

Manohar, V.S., Jayasree, K., Kiran, K., Rupa, M.L., Rohit, D., Chandrasekhar, N., 2012. Evaluation of hypoglycaemic and antihyperglycemic effect of freshly prepared aqueous extract of Moringa Oleifera leaves in normal and diabetic rabbits. J. Chem. Pharm. Res. 4, 249–253.

Nahar, S., Faisal, F.M., Iqbal, J., Rahman, M.M., Yusuf, M.A., 2016. Antiobesity activity of Moringa Oleifera leaves against high fat diet-induced obesity in rats. Int. J. Basic Clin. Pharmacol. 5, 1263–1268.

Nova, E., Redondo-Useros, N., Martínez-García, R.M., Gómez-Martínez, S., Díaz-Prieto, L.E., Marcos, A., 2020. Potential of Moringa Oleifera to improve glucose control for the prevention of diabetes and related metabolic alterations: a systematic review of animal and human studies. Nutrients 12 (7), 2050. doi:10.3390/nu12072050.

Olayaki, LA, Irekpita, JE, Yakubu, MT, Ojo, OO., 2015. Methanolic extract of Moringa oleifera leaves improves glucose tolerance, glycogen synthesis and lipid metabolism in alloxan-induced diabetic rats. J. Basic Clin. Physiol. Pharmacol. 26 (6), 585–593. doi:10.1515/jbcpp-2014-0129.

Pardo, P.S., Boriek, A.M., 2011. The physiological roles of Sirt1 in skeletal muscle. Aging (Albany NY) 3 (4), 430–437. doi:10.18632/aging.100312.

Patrizio, F., Ditroilo, M., Felici, F., Duranti, G., De Vito, G., Sabatini, S., Sacchetti, M., Bazzucchi, I., 2018. The acute effect of Quercetin on muscle performance following a single resistance training session. Eur. J. Appl. Physiol. 118 (5), 1021–1031. doi:10.1007/s00421-018-3834-y.

Petr, M., Stastny, P., Zajac, A., Tufano, J.J., Maciejewska, Skrendo, 2018. A. The role of peroxisome proliferator-activated receptors and their transcriptional coactivators gene variations in human trainability: a systematic review. Int. J. Mol. Sci. 19 (5), 1472. doi:10.3390/ijms19051472.

Sabatini, S., Sgrò, P., Duranti, G., Ceci, R., Di Luigi, L., 2011. Tadalafil alters energy metabolism in C2C12 skeletal muscle cells. Acta Biochim. Pol. 58 (2), 237–241.

Sahlin, K., Harris, R.C., 2011. The creatine kinase reaction: a simple reaction with functional complexity. Amino Acids 40 (5), 1363–1367. doi:10.1007/s00726-011-0856-8.

Saucedo-Pompa, S., Torres-Castillo, J.A., Castro-López, C., Rojas, R., Sánchez-Alejo, E.J., Ngangyo-Heya, M., Martínez-Ávilla, G.C.G, 2018. Moringa plants: Bioactive compounds and promising applications in food products. Food Res. Int. 111, 438–450.

Seok, H., Cha, B.S., 2013. Refocusing peroxisome proliferator activated receptor-alpha: a new insight for therapeutic roles in diabetes. Diabetes Metab. J. 37, 326–332. doi:10.4093/dmj.2013.37.5.326.

Sinacore, D.R., Gulve, E.A., 1993. The role of skeletal muscle in glucose transport, glucose homeostasis, and insulin resistance: implications for physical therapy. Phys. Ther. 73 (12), 878–891. doi:10.1093/ptj/73.12.878.

Stec, D.E., Gordon, D.M., Hipp, J.A., Hong, S., Mitchell, Z.L., Franco, N.R., Robison, J.W., Anderson, C.D., Stec, D.F., Hinds Jr., T.D., 2019. Loss of hepatic PPARα promotes inflammation and serum hyperlipidemia in diet-induced obesity. Am. J. Physiol. Regul. Integr. Comp. Physiol. 317 (5), R733–R745. doi:10.1152/ajpregu.00153.2019.

Stohs, S.J., Hartman, M.J., 2015. Review of the safety and efficacy of Moringa Oleifera. Phytother. Res. 29 (6), 796–804. doi:10.1002/ptr.5325.

Xu, W., Miyamoto, L., Aihara, H., Yamaoka, T., Tanaka, N., Tsuchihashi, Y., Ikeda, Y., Tamaki, T., Kashiwada, Y., Tsuchiya, K., 2018. Methanol extraction fraction from Citrus Sudachi peel exerts lipid reducing effects in cultured cells. J. Med. Invest. 65 (3.4), 225–230. doi:10.2152/jmi.65.225.

Watchko, J.F., Daood, M.J., LaBella, J.J., 1996. Creatine kinase activity in rat skeletal muscle relates to myosin phenotype during development. Pediatr. Res. 40 (1), 53–58. doi:10.1203/00006450-199607000-00010.

Wu, Z., Puigserver, P., Andersson, U., Zhang, C., Adelmant, G., Mootha, V., Troy, A., Cinti, S., Lowell, B., Scarpulla, R.C., Spiegelman, B.M., 1999. Mechanisms controlling mitochondrial biogenesis and respiration through the thermogenic coactivator PGC-1. Cell 98, 115–124 10.1016/S0092-8674(00)80611-X..

Yang, C, Aye, CC, Li, X, Diaz Ramos, A, Zorzano, A, Mora, S, 2012. Mitochondrial dysfunction in insulin resistance: differential contributions of chronic insulin and saturated fatty acid exposure in muscle cells. Biosci. Rep. 32 (5), 465–478. doi:10.1042/BSR20120034.

Zanou, N., Gailly, P., 2013. Skeletal muscle hypertrophy and regeneration: interplay between the myogenic regulatory factors (MRFs) and insulin-like growth factors (IGFs) pathways. Cell Mol. Life Sci. 70 (21), 4117–4130. doi:10.1007/s00018-013-1330-4.